



## Synthesis, Spectroscopic Characterization, and Biological Assessment of Novel Benzothiazole Derivatives Bound to Transition Metal Complexes

DEBARAJ B. PALLAI<sup>1</sup>, MELWIN DIEGO DSOUZA<sup>1</sup>, KALIMODDIN I. MOMIN<sup>2</sup>,  
ABHAY S. BONDGE<sup>3</sup>, DADASAHEB D. KADAM<sup>4</sup>, PRASHANT P. BHUJBAL<sup>4</sup>,  
GANPAT R. NAGARGOJE<sup>5</sup>, PRASAD D. KADAM<sup>6</sup>, SHARAD P. PANCHGALLE<sup>7</sup>  
and VIJAYKUMAR S. MORE<sup>8\*</sup>

<sup>1</sup>St. Joseph Vaz College, Cortalim, Goa, 403710, India.

<sup>2</sup>Department of Chemistry, Rajarshi Shahu Mahavidyalaya, Latur, Dist. Latur, Maharashtra, 413512, India.

<sup>3</sup>Department of Chemistry, Shivaneri Mahavidyalaya Shirur Anantpal, Dist. Latur, Maharashtra, 413544, India.

<sup>4</sup>Department of Chemistry, Narayanrao Waghmare Mahavidyalaya, Akhada Balapur, Dist. Hingoli, Maharashtra, 431701, India.

<sup>5</sup>Department of Chemistry, Shivaji Mahavidyalaya, Renapur Dist. Latur, Maharashtra, 413527, India.

<sup>6</sup>Department of Chemistry, Shri Kumarswami Mahavidyalaya, AUSA, Dist. Latur, Maharashtra, 413520, India.

<sup>7</sup>Department of Chemistry, K. M. C. College, Khopoli, Dist. Raigad, Maharashtra, 410203, India.

<sup>8</sup>Department of Chemistry, Kai. Rasika Mahavidyalaya Deoni, Dist. Latur, Maharashtra, 413519, India.

\*Corresponding author E-mail: vijaymore@gmail.com

<http://dx.doi.org/10.13005/ojc/400324>

(Received: January 25, 2024; Accepted: May 23, 2024)

### ABSTRACT

A range of metal complexes derived from the HBTADH ligand (4-[[6-chloro-1,3-benzothiazol-2-yl]imino]methyl]benzene-1,4-diol) have been synthesized, and their structural characterization has been conducted, yielding compounds of the type  $[M(BTADH)_2]$ . Electron spin resonance (ESR), electronic absorption, mass, electromagnetic moments, NMR, infrared, and C, H, N, and S analysis spectroscopy were some of the methods used for characterization. A tetrahedral geometry has been projected for the complexes containing Hg(II), Zn(II), and Cd(II), but a high spin octahedral geometry is anticipated for the other complexes. In contrast, the spectra suggest that the Pd(II) complex will have a square planar shape. Metal complexes in nitrobenzene do not behave like electrolytes because of the compound's low molar conductance values. In addition, this study examined and evaluated the antibacterial activity of all compounds that were synthesized.

**Keywords:** Octahedral geometry, Metal complexes, Square planar, Tetrahedral, and Biological activity.



## INTRODUCTION

Since their first identification by Schiff in 1864, the products of condensation between carbonyl compounds and primary amines are known as Schiff bases<sup>1-3</sup>. Schiff bases have found several applications in various fields, including analytical chemistry, catalysis, the food industry, fungicidal agents, agrochemicals, and biological activity<sup>4</sup>. The need for innovative, highly effective antimicrobials with few unwanted side effects is rising in response to the rising incidence of deep mycosis<sup>5</sup>.

The benzothiazole ring system is a unique type of bicyclic ring with high significance in the pharmaceutical industry due to its potent biological actions. Compounds containing a simple benzothiazole nucleus are often explored to discover and evaluate products with promising biological activity. The 2-substituted benzothiazole structure, in particular, has gained importance in various therapeutic applications. Changes in the substituent group at the C-2 position can lead to alterations in bioactivity, as evidenced by structure-activity relationship studies<sup>5</sup>.

First synthesized by A. W. Hofmann in 1887, substituted benzothiazole has been the subject of various synthetic methods due to its diverse action and facile cyclization mechanism<sup>6</sup>. Benzothiazoles, with their diverse applications and biological activity, especially anti-tumor, anti-inflammatory, antimalarial, antifungal, anticandidal, and other central nervous system (CNS) actions, have garnered significant attention<sup>7</sup>. Novel benzothiazole derivatives including the azo moiety and associated binuclear metal complexes are the focus of our research. We aim to synthesize, characterize, and evaluate their biological activity. This work aligns with our interest in the synthesis of benzothiazole derivatives.

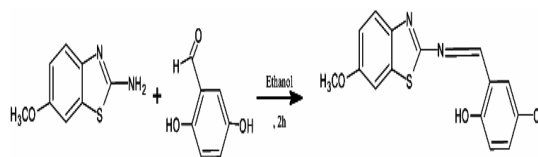
## MATERIALS AND METHODS

Merck, BLD Pharma, and Sigma-Aldrich supplied the solvents and reagents. The HBTADH and its metal complexes have their hydrogen, carbon, nitrogen, and sulfur percentages determined using the Perkin Elmer 24°C elemental analyzer. The Bruker IMPACT HD mass spectrometer was used for the mass spectrometry analysis. A nuclear magnetic resonance (NMR) spectrometer from Bruker,

calibrated with trimethylsilyl, was used to record the spectra of the HBTADH ligand. With the help of a JASCO V650 UV-Visible spectrophotometer, electronic absorption spectra were captured in DMF. An FT-IR spectrometer from Bruker was used to acquire KBr pellet FT-IR spectra. We used a Gouy balance to quantify the complexes' magnetic moments with  $\text{Hg}[\text{Co}(\text{NCS})_4]$  as a standard, and we used Pascal's constants to establish diamagnetic corrections. Using a Q band ESR Spectrometer, ESR spectra were acquired at room temperature. The instrument in question is the JES-FA200. An examination using powder XRD was carried out using BRUKER D8 VENTURE equipment that utilized Cu-K $\alpha$  radiation.

## Synthesis of HBTADH ligand

Scheme 1 shows the process for developing the HBTADH ligand. The 6-methoxy-2-aminobenzothiazole solution, which was 10 mM ethanolic, was stirred using a magnetic stirring rod in a round-bottom flask. Afterwards, a 1:1 ratio of 2,4-dihydroxybenzaldehyde ethanolic solution (10 mM) was added dropwise. Using TLC, the RM was agitated continuously at 50-60°C for 2 hours. It was then necessary to cool the mixture to room temperature before isolating and purifying the solid result, which had a yellow hue, using cold ethanol and petroleum ether washes. Vacuum drying using desiccators containing anhydrous  $\text{CaCl}_2$  was applied to the Schiff bases.



Scheme 1. Preparation of HBTADH

## Synthesis of metal (II) complexes

While stirring a 20 mM hot ethanolic solution of HBTADH ligand, a hot ethanolic solution of metal sulfates (10 mM) was gradually added drop by drop, resulting in the development of color in the solution. The pH level was adjusted to 7 using a dilute alkali. The solid obtained was filtered and underwent successive washes with hot ethanol to eliminate any impurities. The metal complexes were then dried in vacuum desiccators with anhydrous  $\text{CaCl}_2$  added.

## Antimicrobial activity

The antibacterial efficacy of the HBTADH

ligand and its complexes was assessed through the disc diffusion technique on a nutrient agar medium<sup>21-22</sup>. Antibacterial activity was evaluated *in vitro* for bacteria. The medication solution was left to soak into the plate for one hour to improve diffusion. After a 24-h incubation period at 37°C for bacteria and 48 h for fungus, the plates were examined for the zone of inhibition in mm. The molecule that inhibited bacterial growth was determined after 24 h of incubation at 37°C in terms of concentration ( $\mu\text{g/mL}$ ). It's noteworthy that none of the microorganisms tested were influenced by variations in DMSO content in the medium.

### *In vitro* cytotoxicity

Investigated for cytotoxicity through a brine shrimp bioassay, the synthesized HBTADH ligand, and complexes were examined<sup>23</sup>. With 38 g of sodium chloride to 1000 milliliters of tap water, half of a tank was previously filled with salt water, and prawn eggs were added. The eggs hatched into nauplii within 48 h, and the newborn shrimp were collected for the bioassay. Test tubes containing different amounts of dried complexes (2.5, 7.5, 10, and 12.5 mg/10 mL) were prepared, and their cytotoxic potential was assessed by dissolving DMSO in them.

To ensure accurate findings for the cytotoxic activity of the drug, every test tube was supplied with 10 live prawns through a Pasteur pipette. To ensure the reliability of the testing method, a control group was incorporated. After one day, the tubes were microscopically examined to record any pertinent observations and count the number of nauplii that survived. Each experiment consisted of three sets of five replicates. From the

collected data, the  $\text{LC}_{50}$ ,  $\text{LC}_{90}$ , 95% confidence limit, and chi-square were computed. Abbott's method<sup>24</sup> was employed to adjust the data, accounting for control fatalities with the formula % deaths = [(test-control)/control] x 100.

## RESULTS AND DISCUSSION

The HBTADH ligand and its metal complexes exhibit color and stability when stored at room temperature. A wide range of organic solvents, including chloroform, methanol, acetonitrile, DMSO, DMF, and DCM, are compatible with HBTADH ligands. The complexes exhibit solubility in dimethyl sulfoxide (DMSO), and nitrobenzene (DMF), and not aqueous whatsoever. Analytical data for all synthesized complexes align well with the anticipated values for 1:2 metal-to-ligand stoichiometric ratios. The prepared complexes measured molar conductance's at room temperature in nitrobenzene ( $10^{-3}$  M solutions). Table 1's results point to the fact that they are not electrolytic<sup>25</sup>.

The HBTADH ligand and its metal complexes exhibit color and stability at room temperature. Various organic solvents, including methanol, acetonitrile, chloroform, DMSO, DMF, and DCM, are compatible with HBTADH ligands. The compounds are insoluble in water but dissolve in dimethyl sulfoxide, nitrobenzene, and dry mass solid solvents. Analytical data for all synthesized complexes align well with the anticipated values for 1:2 metal-to-ligand stoichiometric ratios. Table 1 shows that the complexes were not electrolytic when their molar conductance was measured at room temperature in nitrobenzene ( $10^{-3}$  M solutions)<sup>25</sup>.

**Table 1: Analytical and physical data of prepared compounds**

Compounds	Color	MW	% Yield	MP/DP	Element Content						Cond	MM
					M	C	H	N	O	S		
HBTADH	Yellow	300.33	86.45	183	-	59.99	4.03	9.33	15.98	10.68	-	-
Fe(BTADH) <sub>2</sub>	Blue	654.55	93.15	201	8.54	55.05	3.36	8.56	14.68	9.79	1.87	5.57
Co(BTADH) <sub>2</sub>	Brown	659.65	80.30	203	8.94	54.57	3.34	8.49	14.60	9.70	1.59	4.96
Ni(BTADH) <sub>2</sub>	Orange	659.35	79.88	202	8.90	54.60	3.34	8.49	14.60	9.71	0.72	3.00
Pd(BTADH) <sub>2</sub>	Red	706.66	84.98	208	15.00	50.94	3.11	7.93	14.60	9.06	0.22	-
Cu(BTADH) <sub>2</sub>	Green	664.21	74.10	205	9.57	54.20	3.31	8.43	14.50	9.64	2.28	1.91
Zn(BTADH) <sub>2</sub>	Yellow	666.05	82.28	208	9.82	54.05	3.30	8.41	14.40	9.61	0.89	-
Cd(BTADH) <sub>2</sub>	Yellow	713.07	82.13	211	15.77	50.49	3.09	7.85	13.50	8.98	1.39	-
Hg(BTADH) <sub>2</sub>	Red	800.66	80.86	207	25.05	44.96	2.75	6.99	11.99	7.99	4.25	-
Mn(BTADH) <sub>2</sub>	Brown	653.59	71.63	201	8.41	55.08	3.37	8.58	14.70	9.79	0.38	5.38

### FT(IR) spectroscopy

The FTIR data that correspond to the metal

complexes and ligands can be found in Table 2. In the infrared spectra of the HBTADH ligand, the

phenolic hydroxyl group is represented by a band at 3068 cm<sup>-1</sup>. Phenol hydroxyl group deprotonation, as indicated by its absence in the complex spectra, implies that it participates in bond formation with the metal ions. Because the azomethine group contains  $\nu(>C=N-)$ , the free ligand shows broadband at 1630 cm<sup>-1</sup> in its infrared spectra. Within complexes, this band moves to 1537–1588 cm<sup>-1</sup> as the ligand coordinates with the central divalent metal ions.

free HBTADH ligand spectrum indicates aromatic C-S stretching vibrations, and this vibration shifts to a lower frequency of 1206–1226 cm<sup>-1</sup> upon complexation, signifying bonding of the sulfur (aromatic) group of the HBTADH ligand to the metal ions. Additionally, newly observed bands between 537-635 cm<sup>-1</sup> and 535-599 cm<sup>-1</sup> are attributed to N-N and S-M, while those between 510 and 555 cm<sup>-1</sup> are attributed to O-M. Imino nitrogen, aromatic sulfur, and phenolic oxygen atoms are confirmed to be coordinated with metal ions by the FTIR spectra.

The prominent band at 1252 cm<sup>-1</sup> in the

**Table 2: Spectral data from FT(IR) analysis of the HBTADH ligand and its metal complexes**

Compounds	-OH(C4)	-OH(C2)	-OCH <sub>3</sub>	-C-H=	>C=N-	C-O	Ar -OH	C-S	N→M	S→M	O-M
HBTADH	3349	3068	2943	2830	1630	1328	1265	1252	-	-	-
Fe(BTADH) <sub>2</sub>	3350	-	2920	2848	1571	1362	1265	1212	635	538	517
Co(BTADH) <sub>2</sub>	3562	-	2924	2835	1537	1390	1279	1222	629	599	555
Ni(BTADH) <sub>2</sub>	3350	-	2921	2850	1578	1309	1266	1215	590	571	532
Pd(BTADH) <sub>2</sub>	3350	-	2922	2850	1565	1312	1264	1215	582	-	530
Cu(BTADH) <sub>2</sub>	3391	-	2921	2850	1580	1308	1263	1214	567	535	516
Zn(BTADH) <sub>2</sub>	3381	-	3187	2796	1588	1316	1226	1226	544	-	518
Cd(BTADH) <sub>2</sub>	3195	-	2981	2836	1583	1324	1252	1215	602	-	551
Hg(BTADH) <sub>2</sub>	3399	-	2920	2850	1566	1314	1263	1222	537	-	510
Mn(BTADH) <sub>2</sub>	3352	-	2920	2849	1568	1338	1274	1206	611	552	541

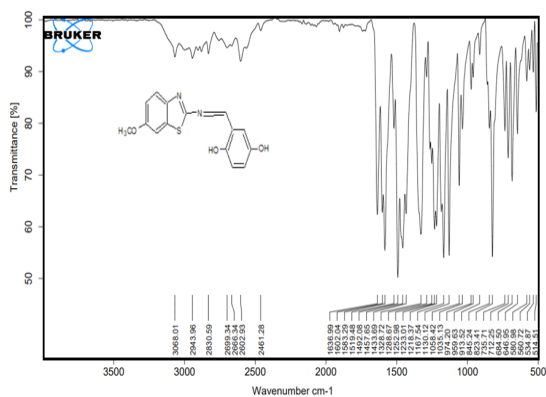


**Fig. 1. IR spectrum of the HBTADH ligand**

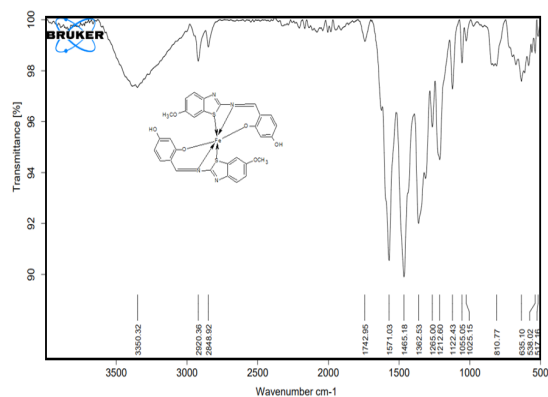


**Fig. 2. IR spectrum of the [Fe(BTADH)<sub>2</sub>] complex**

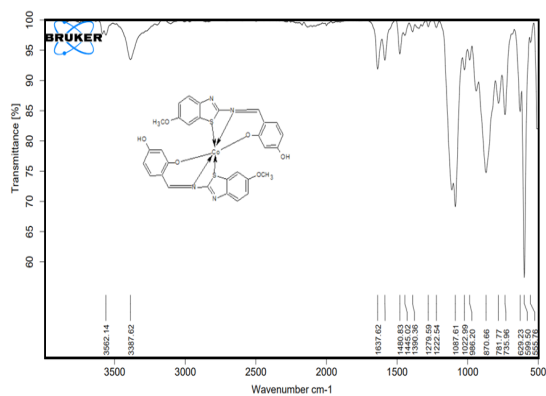


**Fig. 3. IR spectrum of the [Co(BTADH)<sub>2</sub>] complex**

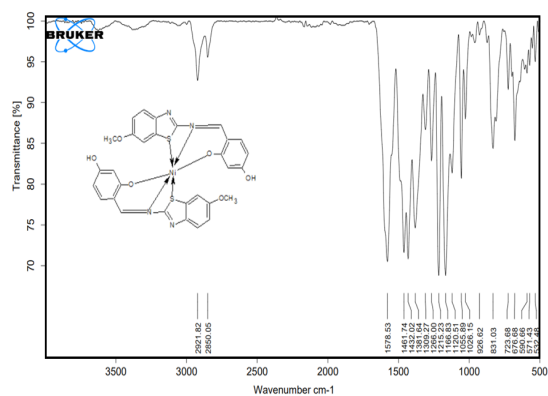


**Fig. 4. IR spectrum of the [Ni(BTADH)<sub>2</sub>] complex**

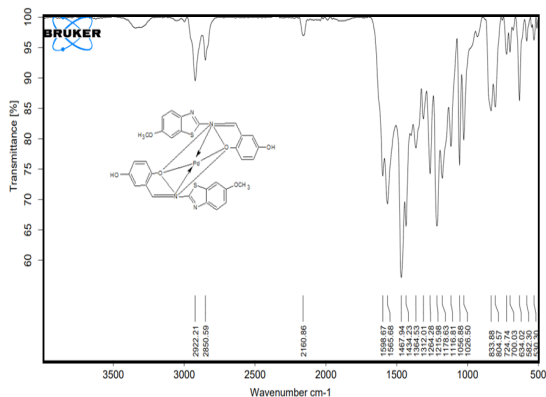


Fig. 5. IR spectrum of the [Pd(BTADH)<sub>2</sub>] complex

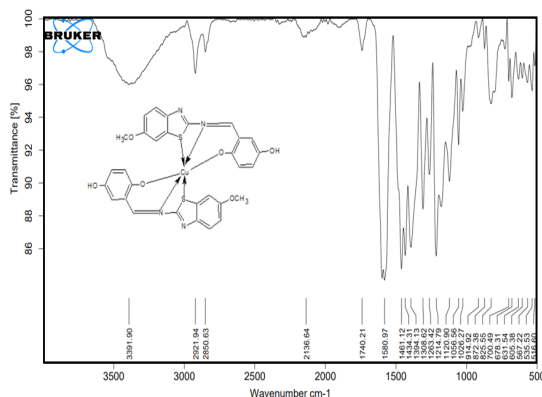


Fig. 6. IR spectrum of the [Cu(BTADH)<sub>2</sub>] complex

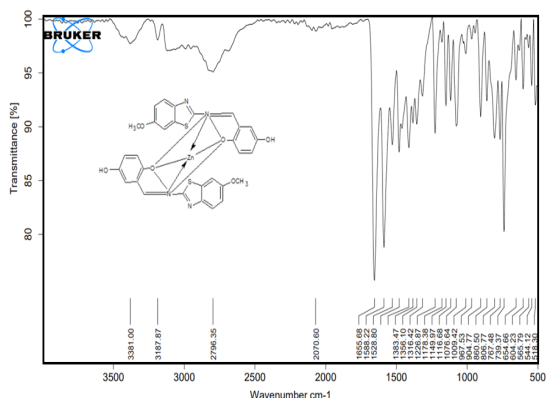


Fig. 7. IR spectrum of the [Zn(BTADH)<sub>2</sub>] complex

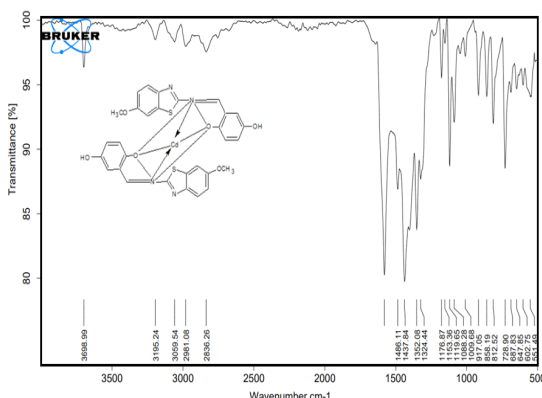


Fig. 8. IR spectrum of the [Cd(BTADH)<sub>2</sub>] complex

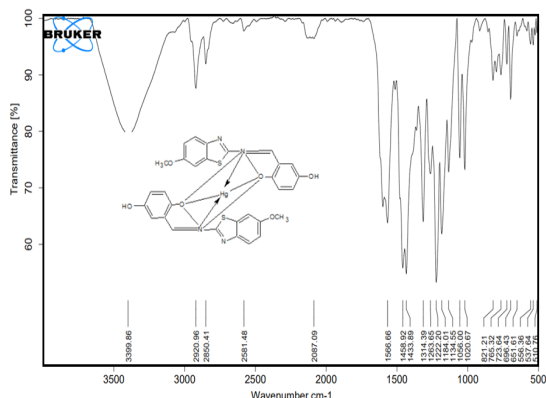


Fig. 9. IR spectrum of the [Hg(BTADH)<sub>2</sub>] complex

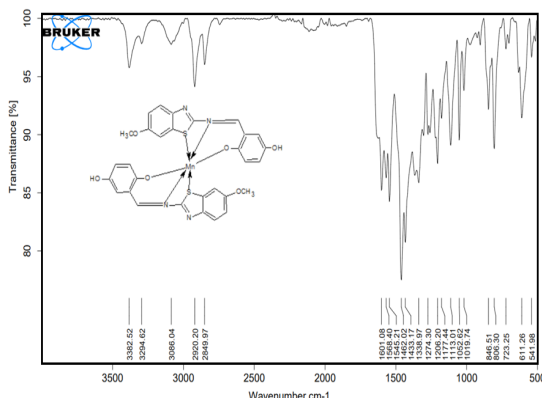


Fig. 10. IR spectrum of the [Mn(BTADH)<sub>2</sub>] complex

**ESR spectra**

The ESR spectrum of the [Cu(BTADH)<sub>2</sub>] complex offers essential insights into the degree of electron delocalization and the character of the metal-ligand interaction. Values of  $g_{||}$ , 2.08, and 1.51 were found via spectral analysis, in that order. A deformed octahedral geometry is shown by the greater  $g_{||}$  value relative to  $g_{\perp}$  in the [Cu(BTADH)<sub>2</sub>] complex. In addition, the complex is in a <sup>2</sup>B<sub>1g</sub> ground state because an unpaired

electron is located in the  $d_{x^2-y^2}$  molecular orbital. The designation "G" signifies significant trade contacts across copper centers<sup>34</sup>.

The g-value, obtained from references<sup>35,36</sup>, is below 2.3, indicating a covalent connection between the metal and ligand. This information contributes to a comprehensive understanding of the electronic structure and coordination environment of the [Cu(BTADH)<sub>2</sub>] complex.

**UV-Visible spectra and Magnetic moments**

Electronic spectra measured in DMF solutions are summarized in Table 4. There was an increase in energy absorption between 445 and 285 nm, known as a charge transfer band, in every single compound.

An octahedral structure containing five unpaired electrons gives the Fe(II) complex an effective magnetic moment of 5.57 BM<sup>57</sup>. The existence of absorption bands at 585 nm in the electronic spectra, which correspond to the  ${}^5T_{2g} \rightarrow {}^5E_g$  electronic transition, allowed for the confirmation of an octahedral structure for the iron(II) complex<sup>51</sup>.

According to the  ${}^4T_{1g}(F) \rightarrow {}^4T_{1g}(P)$   $\nu_3$ ,  ${}^4T_{1g}(F) \rightarrow {}^4A_{2g}(F)$   $\nu_2$ , and  ${}^4T_{1g}(F) \rightarrow {}^4T_{2g}(F)$   $\nu_1$ , transitions, the cobalt(II) complex exhibited *d-d* bands at 435, 635, and 900 nm in its electronic spectra, respectively. The complexes' octahedral shape is supported by these transitions. Three *d-d* transition bands were visible in the absorption spectra of the nickel(II) complex, at 970, 620, and 529 nm. The presence of an octahedral structure with  $D_{4h}$  symmetry is supported by these bands, which correspond to the  ${}^3A_{2g}(F) \rightarrow {}^3T_{1g}(P)$   $\nu_3$ ,  ${}^3A_{2g}(F) \rightarrow {}^3T_{1g}(F)$   $\nu_2$ , and  ${}^3A_{2g}(F) \rightarrow {}^3T_{2g}(F)$   $\nu_1$ , transitions, respectively.

In our analysis of the Ni(II), and Co(II) complexes, we considered several factors, including the ligand field stabilization energy (LFSE), covalency, B, and 10 Dq. The B and Dq values of Co(II) complexes were calculated by taking into account the complexes' covalent nature and applying the 3/1 ratio determined from the transition energy ratio diagram.

According to<sup>50</sup>, absorptions at 490 and 686 nm, which are associated with the transitions  ${}^2B_{1g} \rightarrow {}^2B_{2g}$  and  ${}^2B_{1g} \rightarrow {}^2E_g$ , respectively, in the Cu(II) complex, suggested a deformed octahedral geometry enclosing copper(II). Electronic spectra and magnetic moments provided evidence that the Mn(II) complex was structured octahedrally. According to<sup>55</sup>, the electronic spectra showed bands at 442 and 375 nm, which were associated with  ${}^6A_{1g} \rightarrow {}^3T_{1g}(P)$  and  ${}^6A_{1g} \rightarrow {}^3T_{1g}(F)$  electronic transitions, respectively. The complex's octahedral shape was confirmed by its effective magnetic moment measurement of 5.38 BM<sup>56</sup>.

The spectra of the complex showed three bands, one for each of the three lower *d* orbitals and one for the unoccupied  $d_{x^2-y^2}$  orbital, due to three *d-d* spin-allowed transitions. In the electronic spectra, distinct *d-d* transition bands were observed

at wavelengths of 392 nm, 319 nm, and 283 nm. These transitions were identified as originating from the shifts between  ${}^1A_{1g} \rightarrow {}^1A_{2g}$ ,  ${}^1A_{1g} \rightarrow {}^1B_{1g}$  and  ${}^1A_{1g} \rightarrow {}^1E_{1g}$  energy levels, respectively. These compounds are square and planar, according to the electronic spectra<sup>20</sup>.

**Table 3: The HBTADH ligand and its metal complexes' electronic spectrum**

Compound	nm	Transition
HBTADH	265	$\pi \rightarrow \pi^*$
	283	$\pi \rightarrow \pi^*$
Fe(BTADH) <sub>2</sub>	442	${}^6A_{1g} \rightarrow {}^4T_{1g}({}^4P)$
	375	${}^6A_{1g} \rightarrow {}^4E_g({}^4D)$
Fe(BTADH) <sub>2</sub>	585	${}^5T_{2g} \rightarrow {}^5E_g$
	442, 368, 273	LMCT
Co(BTADH) <sub>2</sub>	900	${}^4T_{1g}(F) \rightarrow {}^4T_{2g}(F) (\nu_1)$
	635	${}^4T_{1g}(F) \rightarrow {}^4T_{2g}(F) (\nu_2)$
Ni(BTADH) <sub>2</sub>	970	${}^3A_{2g}(F) \rightarrow {}^3T_{2g}(F) (\nu_1)$
	620	${}^3A_{2g}(F) \rightarrow {}^3T_{1g}(F) (\nu_2)$
Pd(BTADH) <sub>2</sub>	392, 319, 283	LMCT
Cu(BTADH) <sub>2</sub>	686	${}^2B_{1g} \rightarrow {}^2A_{1g} (\nu_1)$
Zn(BTADH) <sub>2</sub>	392, 307, 384	LMCT
Cd(BTADH) <sub>2</sub>	325, 298	LMCT
Hg(BTADH) <sub>2</sub>	373, 330, 285	LMCT

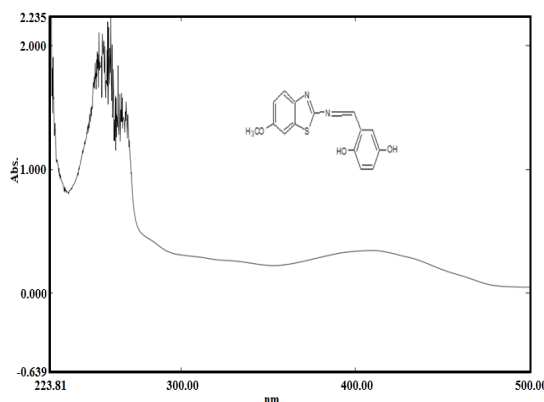


**Fig. 11. UV spectrum of ligand**

**NMR spectra**

Table 4 presents the <sup>1</sup>H NMR spectra (measured in ppm) of both the HBTADH ligand and its corresponding metal complexes dissolved in CDCl<sub>3</sub>. The addition of D<sub>2</sub>O serves to neutralize the acidic phenolic -OH protons at the C2 position ( $\delta$  12.07 ppm) in the HBTADH ligand, indicating the involvement of the hydroxyl group in metal ion interaction.

One peak at  $\delta$ 3.91 ppm (s, 3H, H<sub>3</sub>C-O) is shown in the <sup>1</sup>H-NMR spectra of the ligand HBTADH, originating from the three protons of the methoxy group, one singlet at  $\delta$ 10.74 ppm (s, 1H, Ar-OH, C4), and one singlet at  $\delta$ 9.24 ppm (s, 1H, -CH=) attributable to a methyl group attached to the



the lipophilic characteristic pivotal in antimicrobial activity. Chelation makes complexes more lipophilic by reducing the metal ion's polarity, which in turn promotes electron delocalization across the chelate ring. Many aspects contribute to the efficiency of the complexes, including chelation, concentration, shape, stereochemistry, solubility, hydrophobicity, and coordination sites, among others.

**Table 5: A study on the antimicrobial activities**

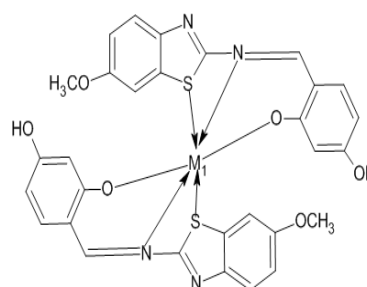
Compound	Antibacterial Activity (zone of inhibition)			
	<i>S. aureus</i>	<i>B. subtilis</i>	<i>E. coli</i>	<i>P. aeruginosa</i>
HBTADH	8	8	12	0
Fe(BTADH) <sub>2</sub>	14	13	18	9
Co(BTADH) <sub>2</sub>	15	9	24	10
Ni(BTADH) <sub>2</sub>	25	21	20	25
Pd(BTADH) <sub>2</sub>	8	14	0	9
Cu(BTADH) <sub>2</sub>	9	8	0	6
Zn(BTADH) <sub>2</sub>	14	8	0	0
Cd(BTADH) <sub>2</sub>	8	12	25	7
Hg(BTADH) <sub>2</sub>	14	8	23	12
Mn(BTADH) <sub>2</sub>	12	19	0	0
Streptomycin	10	7	13	8

### CONCLUSION

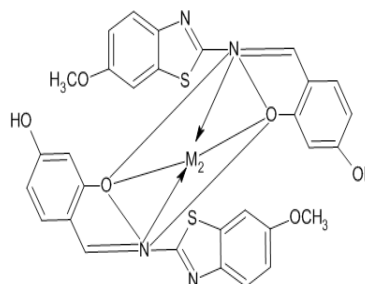
Applying a variety of spectroscopic and analytical methods, mononuclear binary metal(II) complexes were synthesised and characterised from HBTADH. The results indicate that apart from the complex containing Pd(II), all the others have a high spin octahedral structure, tetrahedral geometry for Hg(II), Cd(II), and Zn(II), and square planar geometry for Pd(II). When an azomethine and an oxygen atom from a hydroxyl group join with a metal in a 1:2 ligand stoichiometry, a coordination complex develops.

Against every single bacterium that was

examined, the metal complexes exhibited greater antibacterial activity than the free ligand. Compared to the Co(II) and Ni(II) complexes, the Cu(II) complex exhibited a far stronger antibacterial action. The following are the complicated structures that spectral studies have determined:



Where M<sub>1</sub> = Mn(II), Fe(II), Co(II), Ni(II) and Cu(II)



Where M<sub>2</sub> = Pd(II), Zn(II), Cd(II) and Hg(II)

### ACKNOWLEDGMENT

The Authors are thankful to Riva Industries, 289/Kirwali, Raigad, Maharashtra, India-410201 for providing spectral data and other activity.

### Conflict of interest

The authors assert that there are no conflicts of interest.

### REFERENCES

- Wang, H.; Dai, X. J.; & Li, C., *J. Nature Chemistry*, **2017**, 9(4), 374-378.
- Wady, A. F.; Hussein, M. B.; Mohammed, M. M., *Sch. Int. J. Chem. Mater. Sci.*, **2021**, 4, 46-53.
- Mary, Y. S.; Mary, Y. S.; Krátký, M.; Vinsova, J.; Baraldi, C.; Gamberini, M. C., *Journal of Molecular Structure*, **2021**, 1228, 129680.
- Valentová, J.; Varényi, S.; Herich, P.; Baran, P.; Bilková, A.; Kožíšek, J.; Habala, L., *Inorganica Chimica Acta*, **2018**, 480, 16-26.
- Rahim, N. A. H. A.; Abbas, S. S.; Aljuboori, S. B.; Mahmood, A. A. R., *Research Journal of Pharm and Tech.*, **2021**, 14(8), 4129-4136.
- Qadir, T.; Amin, A.; Salhotra, A.; Sharma, P. K.; Jeelani, I.; Abe, H., *Current Organic Chemistry*, **2022**, 26(2), 189-214.
- Shirvani, P.; Fassihi, A.; Saghale, L.; Van Belle, S.; Debyser, Z.; Christ, F., *Journal of Molecular Structure*, **2020**, 1202, 127344.
- Pathak, N.; Rathi, E.; Kumar, N.; Kini, S. G.; Rao, C. M., *Mini Reviews in Medicinal Chemistry*, **2020**, 20(1), 12-23.
- Kumar, G.; Singh, N. P., *Bioorganic Chemistry*, **2021**, 107, 104608.
- Spassov, D. S.; Atanasova, M.; Doytchinova, I., *Frontiers in Mole. Biosci.*, **2023**, 9, 1405.

11. Min, L. J.; Zhai, Z. W.; Shi, Y. X.; Han, L.; Tan, C. X.; Weng, J. Q.; Liu, X. H., *Phosphorus, Sulfur, and Silicon and the Related Elements.*, **2020**, *195*(1), 22-28.
12. Silva, F.T.; Franco, C. H.; Favaro, D. C.; Freitas-Junior, L. H.; Moraes, C. B.; Ferreira, E. I., *European Journal of Medicinal Chemistry.*, **2016**, *121*, 553-560.
13. Shaikh, F. M.; Patel, N. B.; Sanna, G.; Busonera, B.; La Colla, P.; Rajani, D. P., *Medi. Chemistry Research.*, **2015**, *24*, 3129-3142.
14. Bauer, A.W.; Kirby, W.W.M.; Sherris J.C.; Turck, M., *Am. J. Clin. Pathol.*, **1966**, *45*, 493.
15. Gross, D.C.; De Vay, S.E., *Physiol. Plant Pathol.*, **1977**, *11*, 13.
16. Piro, O. E.; Echeverría, G. A.; Navaza, A.; Güida, J. A., *Inorganica Chimica Acta.*, **2020**, *511*, 119831.
17. Akıyan.; Özdemir, R.; Ö ütcü, H., *Synthesis and Reactivity in Inorganic, Metal-Organic, and Nano-Metal Chemistry.*, **2014**, *44*(3), 417-423.
18. Özkan, E. H.; Kizil, H. E.; akiyan.; Nartop, D.; Nur en, S. A. R. I.; Güleray, A. A. R. Gazi University *Journal of Science.*, **2018**, *31*(2), 408-414.
19. Diaddario, L. L.; Robinson, W. R.; Margerum, D. W., *Inorganic Chemistry.*, **1983**, *22*(7), 1021-1025.
20. Heinert, D.; Martell, A. E., *Journal of the American Chemical Society.*, **1963**, *85*(2), 188-193.
21. Aly, G. Y.; Rabia, M. K.; Al Mohanna, M. A., *Synthesis and Reactivity in Inorganic and Metal-Organic Chemistry.*, **2004**, *34*(1), 45-66.
22. Singh, G.S.; Pheko, T., *Spectrochim. Acta, Part A.*, **2008**, *70*, 595-600.
23. Wehrli, F.W.; Marchand, A.P.; Wehrli, S. Interpretation of Carbon-13 NMR Spectra; Wiley: New York, USA., **1988**.